

The Application of a Triangular Mesh for Gravity Inversion to Reconstruct Subsurface Geological Structures in the Hululais Geothermal Prospect, Bengkulu

Tofan Sastranegara, Sotarduga S. Nainggolan, and Imam B. Raharjo

PT Pertamina Geothermal Energy, Skyline Building 15th Floor, Jl. MH Thamrin 9th Jakarta, Indonesia 10340

rmtofans@pertamina.com

Keywords: gravity, faults, inversion, triangular mesh, Tompaso

ABSTRACT

Inversions of gravity data need an appropriate initial model in order to guide the process to produce a reasonable subsurface model. Downhole data from wells, such as lithology and density logs, are useful for constructing the initial model in order to constrain the inversion results. Second vertical derivatives (SVD) are also useful in giving additional information, especially to delineate the fault type and its orientation. Based on this information, an inversion domain consisting of a triangular mesh is constructed. The triangles inside the domain are tailored to the fault orientation and location. It is endeavored that this will increase the possibility of constructing an inversion geometry result that matches the geometry of the fault. These inversions, using conjugate gradient algorithms, have been tested to a synthetic model and showed an improvement in reconstructing the density structure distribution of the original model compared to a rectangular mesh. The triangular mesh inversion was applied to gravity data in the Hululais geothermal prospect. The residual map anomaly varies from -22 to 22 mGal in the prospect area as characterized by the existence of low gravity anomalies. It is estimated that the faults are mainly striking in the NW-SE and N-S directions. The density model with a triangular mesh inversion in the line perpendicular to the prospective area showed a subsurface density structure distribution with high-low-high density value associated with the depression structure of the Sumatra Fault. The plane of fault is estimated to have an 80° dip. It provides pathways to the thermal manifestations at the surface.

1. INTRODUCTION

The gravity method is one of the geophysical methods used to measure the variation of the gravitational field at the surface caused by density contrasts within the rocks. We can predict the location, geometry, and density contrast in the subsurface by inverting the gravitational field. Unlike other geophysical methods, gravity inversion has a nonunique solution because an infinite number of object geometries, depths and density contrasts can yield the same anomaly. Additional information, such as the fault dip, is useful in improving the inversion process.

In this study, the second vertical derivative (SVD) from the Bouger anomaly was used to estimate the fault dip. This information was used to reconstruct the orientation of triangular meshes, so that the dip of the triangular mesh is consistent with the results of the SVD analysis. In this approach, nonunique solutions will be constrained and the result will be more realistic from the geological and geophysical perspectives.

2. METHOD

2.1 2D Gravity Inversion

In order to calculate the anomaly of a 2D density distribution, a triangular mesh grid is constructed. The subsurface domain is divided into a triangular mesh, so that the gravity effect in the surface (g) due to the triangular mesh with density values at every observation point (Figure 1) can be calculated in the matrix form using the following equation:

$$g = A\rho \quad (1)$$

The kernel matrix of the forward operator, A , can be calculated in accordance with the Blakely (1995) formula:

$$A = G \sum_{n=1}^{n=3} \frac{\beta_n}{1 - \left(\frac{x_{n+1} - x_n}{z_{n+1} - z_n} \right)^2} \left[\log \frac{r_{n+1}}{r_n} - \frac{x_{n+1} - x_n}{z_{n+1} - z_n} (\theta_{n+1} - \theta_n) \right] \quad (2)$$

where, x_{n+1} and x_n are the geometrical coordinates of x in the first and second points of side n in the triangular mesh and z_{n+1} and z_n are the coordinates of z. In this case, ρ is unknown when A and g are known. Equation 1 can be rewritten as:

$$\rho = (A^T A)^{-1} A^T g \quad (3)$$

Here, ρ can be determined. Equation 3 is the general solution for the inversions.

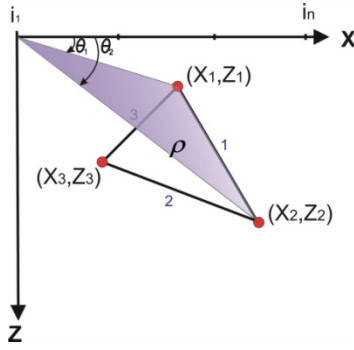


Figure 1. Geometrical conventions used in expressions for the x- and z components of the gravitational acceleration at the origin due to a triangular mesh of density ρ .

2.2 Second Vertical Derivative for Initial Fault Assessment

The purpose of the application of the second vertical derivative (SVD) method to gravity data is to identify the fault type and to estimate fault dipping. The criteria used for determining whether a fault is normal or reverse are as follows:

$$\left| \frac{\partial^2 \Delta g}{\partial^2 z} \right|_{\min} < \left| \frac{\partial^2 \Delta g}{\partial^2 z} \right|_{\max} \text{ for normal faults} \quad (4)$$

$$\left| \frac{\partial^2 \Delta g}{\partial^2 z} \right|_{\min} > \left| \frac{\partial^2 \Delta g}{\partial^2 z} \right|_{\max} \text{ for thrust faults} \quad (5)$$

The response of the gravity anomaly in various dip values for the fault with a density body of 150 kg/m^3 has been simulated and shown in Figure 2. The original model (bottom) has a 40° dip with the model response and the corresponding SVD (blue) response is also shown. It turns out that the curves that delineate the fault interface is located at points where the SVD is zero. The dip is then simulated from 20° up to 90° . Faults with $20^\circ, 30^\circ, 40^\circ, 50^\circ, 60^\circ, 70^\circ, 80^\circ$, and 90° dip values were simulated. Then, the SVD response for each dipping fault was calculated, so that the $|SVD|_{\max}$ and $|SVD|_{\min}$ for each dipping fault can be determined. The corresponding response curves are shown in Figure 2. The linear relationship between the differences of the absolute maximum SVD and absolute minimum SVD to the angle of fault dip is shown in Figure 3. In the case of normal faults, the differences are positive (+) and the value of the normalized SVD is close to zero if the dip of the fault plane is nearly 90° .

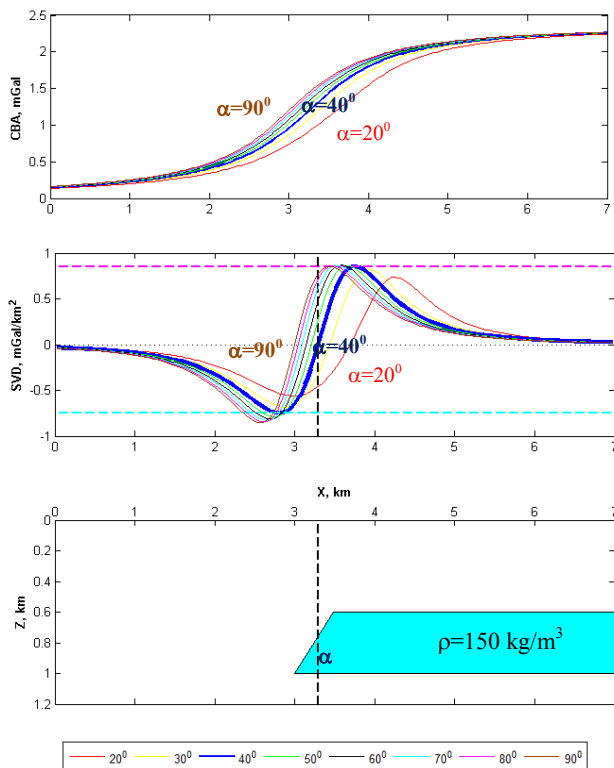


Figure 2. Response of gravity anomaly (top) and SVD (middle) generated from normal fault models with various dip values.

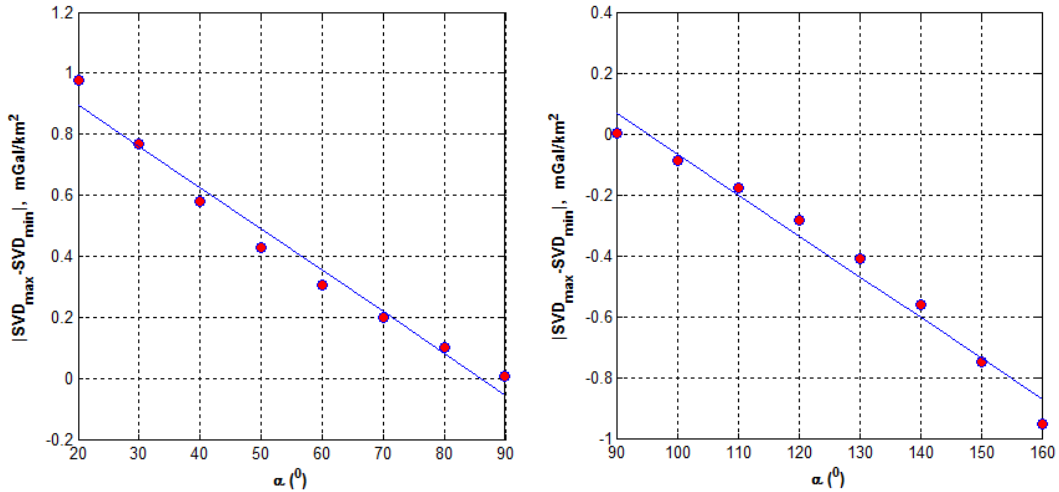


Figure 3. The linear relationship between differences of the absolute maximum SVD and absolute minimum SVD (normalized) to the angle of fault: normal fault (left) and thrust fault (right).

3. SYNTHETIC MODEL EXAMPLE

The triangular mesh inversion was tested for a synthetic model. This method was compared to the conventional method (rectangular mesh inversion), in order to observe the improvement and the efficiency of this method. In this example, subsurface density bodies with dimension $14 \times 4 \text{ km}^2$ were built (Figure 4). The model consisted of two bodies, one is representative of the footwall that has a contrast density of 300 kg/m^3 and the other body (hanging wall) has density contrast 0 kg/m^3 . The fault had a dip value of around 65° .

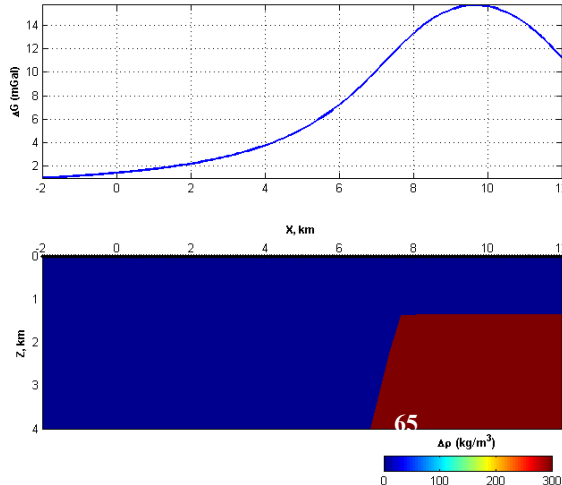


Figure 4. Subsurface density model and gravity data response

In the first inversion scheme, the subsurface density was represented by 20×5 blocks with dimensions of $14 \times 4 \text{ km}^2$ (Figure 5). The initial model of inversion had a homogenous region with zero density (kg/m^3). A misfit of 0.0005 was used, together with the constrain density (-50 to 350 kg/m^3) as an exit criterion. The conjugate gradient algorithm was used as the solution for the inversion. The rectangular mesh inversions yielded a rather poor result. The method was unable to recover the original model both in terms of the geometry and density values. It was difficult to determine the boundary of the fault. This was possibly caused by the dimensional limitation of the mesh, so that density value will be false and will have incorrect geometry.

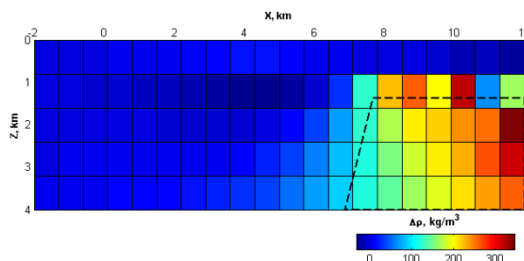


Figure 5. The result of rectangular mesh inversion. The black line denoted original geometry of the model

For the second inversion scheme, SVD analysis was performed before the inversion to guide the construction of the triangular mesh. As shown in Figure 6, the value of the absolute maximum SVD (1.7) is much higher than the absolute minimum value (0.9). Thus, it was concluded that fault type of the model was a normal fault and the angle of dip was less than 90° . To estimate the fault dip more precisely, the normalized amplitude of SVD curves was calculated $((|SVD|_{\max} - |SVD|_{\min}) / (|SVD|_{\max} + |SVD|_{\min}) = (1.7-0.9)/(1.7+0.9)=0.29$. By using the relationship curve between dip angle and normalized $|SVD|_{\max}$ and $|SVD|_{\min}$ in Figure 3, the dip angle of the fault was estimated to be 65° . The fault interface at $x=7.2$ km was characterized by having a zero SVD value in the curve. This information was used to reconstruct the geometry of the mesh in the estimated fault interface. Moreover, the mesh in the outer layer of the estimated fault interface could be constructed independently. However, careful attention must be paid to the mesh in the estimated fault interface that will become the boundary of the fault in inversion result. In this triangular mesh inversion, the same parameters from the inversion process of the rectangular mesh was used. The inversion method performed well, where regular density bodies were centered on the boundary and the calculated values were close to original density values (300 kg/m^3) (Figure 7).

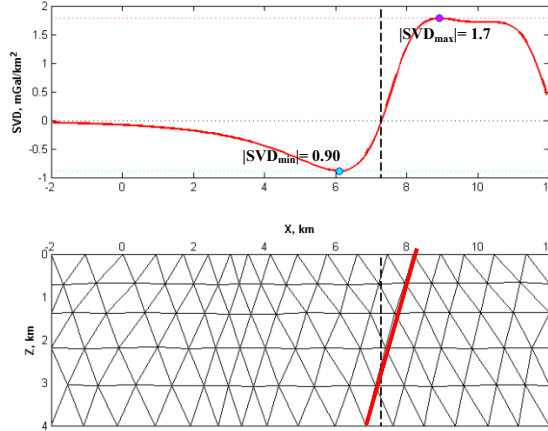


Figure 6. SVD analysis from gravity data to define fault position and angle of fault dip (top). Constructing mesh triangular based on SVD analysis result (bottom).

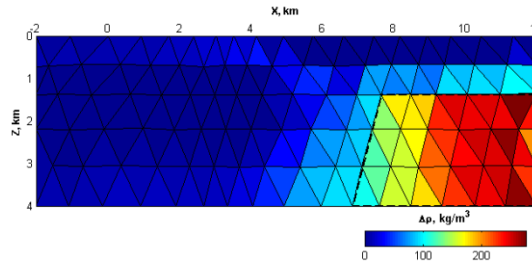


Figure 7. The result of the triangular mesh inversion. The black line denoted original geometry of the model

The synthetic simulation exhibits the importance of building the geometry of the mesh in inversion to be as close as possible to the real geometry of the subsurface density bodies. It guides the inversion result to restore the original density bodies in terms of the geometry and density values. Additional information such as lithology or density logs are also useful in improving the inversion result.

4. REAL DATA

4.1 Gravity Data Acquisition and Processing

The Gravity survey was conducted in 2014 by Pertamina Geothermal Energy Company using three Scintrex CG-5 gravimeters and Total stations for elevation correction. The survey area was about 300 km^2 with a total of 385 gravity stations located along several lines with about 0.25 km spacing and a line interval of about 3 km . A density of 2650 kg/m^3 from the Parasnis method analysis was used to define the Bouguer anomaly. A first order of polynomial was used to produce a regional map. By subtracting the Bouger anomaly and regional map anomaly, the residual map anomaly can be defined. Thus, the gravity anomaly due to density bodies at shallower depths can be enhanced (Telford, 1974). This map was used to model the triangular mesh inversion.

The residual map anomaly (Figure 8) varied from -22 to 22 mGal, where the lowest anomaly (-22 mGal) was estimated as upflow zone of the Hululais geothermal system. There were several changes in the gravity anomaly whose trends were NW-SE and nearly N-S, which were predicted as fault structures. SVD was applied in order to determine a more accurate boundary of the fault. This map showed that the zero contour anomaly of SVD correlated with the trend of the estimated fault structures marked by the presence of manifestations on the surface. By analyzing this map, it was estimated that there were 11 faults (L1-L8 & X1-X3) in this geothermal field. Some of these estimated faults were confirmed by the presence of microearthquake events (MEQ) clustered between faults L7 and L8; and total loss circulation (TLC) in the some wells that were estimated the have crossed fault L5. Triangular mesh inversion was applied to section A-B in order to describe the distribution of subsurface density bodies and display some of the estimated faults vertically.

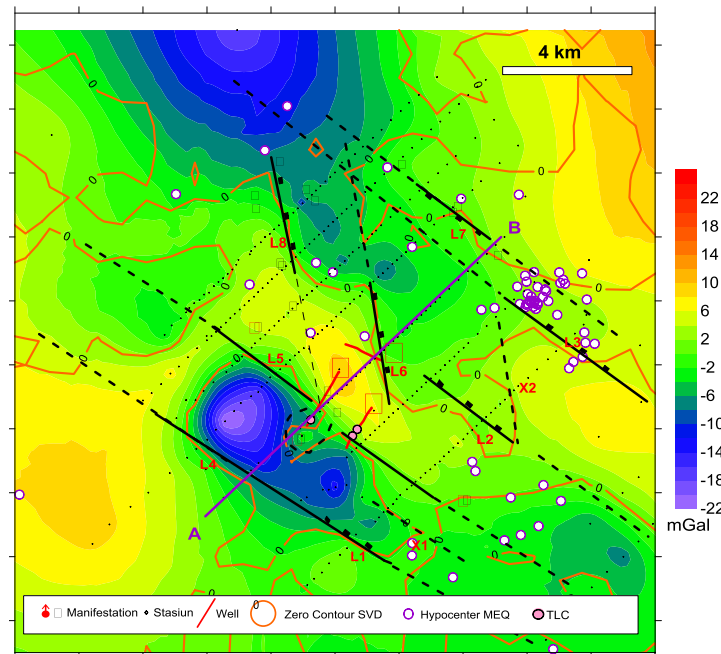


Figure 8. Residual anomaly of the Hululais geothermal field overlain with the zero SVD contour.

4.3 Modelling

A triangular mesh has been constructed to invert the residual gravity data (AB line) in order to confirm the presence of the faults estimated by geology (Figure 9). The triangles inside the domain are tailored to the fault orientation in this area, which are mainly dipping nearly 80° (based on geological information and SVD analysis). Homogenous densities (100 kg/m^3) were used in the initial model. The density range interval of -300 to 300 kg/m^3 were utilized as constraints for the inversion result. The inversion was finished after the minimum misfit was reached and the response of the model to the surface was close enough to the observations and measurements in the field.

The model showed a high-low-high anomaly pattern, which might possibly be associated with the depression structure of the Sumatera fault. Lower densities (-400 kg/m^3) in the left section of the model indicated hydrothermal activities in the geothermal field. The plane of fault was estimated to have dip values of around 80° . It provided pathways to the thermal manifestations at the surface. It was estimated that one of the wells crossed the estimated fault at L5 and X3.

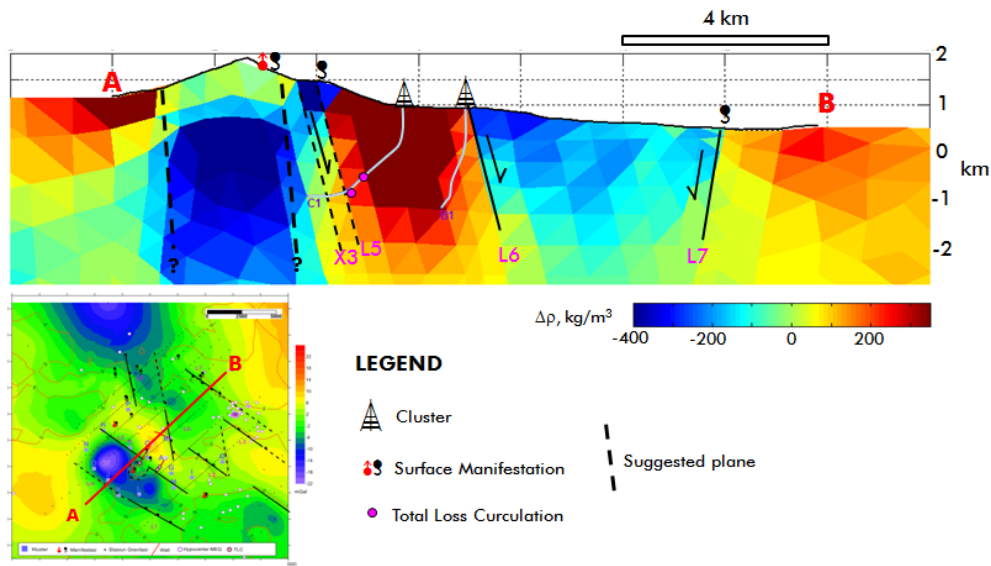


Figure 9. Model subsurface density results from the triangular mesh inversion in the Hululais Geothermal Field.

5. CONCLUSIONS

Triangular mesh inversion was successfully applied to both synthetic and real data. It was demonstrated that the improvements in the geometry of mesh in inversion resulted to density values that were better compared to the results of the rectangular method. Application to a real data set likewise showed that there were some faults in section A-B whose dip values were about 80° . The presence of these faults was validated with the existence of thermal manifestations at the surface, MEQ events clustered at the estimated fault, and TLC at certain depths of the well that were estimated to have crossed the fault.

REFERENCES

Blakely, R.J., 1995, Potential Theory in Gravity and Magnetic Applications: Cambridge University Press.

Telford, W.M. et al: Applied Geophysics, Cambridge University Press, Cambridge (1974)